




## Unidirectional T-splines for Automotive Local-Feature-Lines Modeling Enhanced by Isogeometric Analysis

Xiang Xue<sup>1</sup> 

<sup>1</sup>Nanjing Polytechnic Institute, [njxuexiang@126.com](mailto:njxuexiang@126.com)

Corresponding author: Xiang Xue, [njxuexiang@126.com](mailto:njxuexiang@126.com)

**Abstract.** Local-Feature-Line (LFL) modeling is essential for car-body styling design with the capability of expressing the designer's aesthetic intention and sense. In this paper, we present a new LFL modelling approach based on unidirectional T-spline surface (UT-splines) and isogeometric analysis (IGA). UT-splines is a subset of T-spline surface (T-splines) and can be applied to efficiently build the LFL with a simple surface structure and local refinements. We also incorporate thin-shell mechanical property into UT-splines through IGA to produce an UT-splines+, which seamlessly integrates together the design model and analysis model. In this way, we can employ the analysis model within UT-splines+ to flexibly modify the LFL into a desirable shape through intuitive mechanical editing, saving a lot of time as in geometric editing that commonly requires laborious adjustments of control points. Moreover, we can easily achieve the simultaneous engineering analysis during LFL modeling also based on UT-splines+ without needing the costly meshing process, which greatly facilitates automotive styling design for engineering designers. Finally, a case study about car bonnet design is investigated in details to prove the effectiveness of our new modeling approach in practical application.

**Keywords:** T-splines, Unidirectional T-splines, Isogeometric analysis, Feature-lines modeling, Car-body design

**DOI:** <https://doi.org/10.14733/cadaps.2023.826-838>

### 1 INTRODUCTION

In the highly competitive automotive industry, ever-changing consumer demands are forcing automakers to constantly develop new ways to deliver better products within a shorter period of time. The automobile vehicle not only needs to possess a reliable and safe car-body structure, but also requires to have an aesthetically pleasing appearance of car-body. Hence, styling design in computer aided design (CAD) and engineering analysis in computer aided engineering (CAE) both important for automotive design. Normally, designers adopt freeform surface models, such as Bezier surface, B-spline surface and non-uniform rational B-spline spline (NURBS) surface, in car-body styling design to express their specific tastes in design aesthetics. For example, Bezier

surfaces are applied in ICEM Surf [13] to create high-quality surface models for automotive development. NURBS surfaces are used in Alias Auto [1] to facilitate the freeform surface modeling in car-body design, and are also applied in Rhino3D [23] to define and build complex automotive designing models.

Local-Feature-Lines (LFL) are essential for car-body styling design at the early stage of automotive development [2], because they are good at expressing designer's unique aesthetic intention for car-body appearance. In general, LFLs are defined as local sharp lines along the isocurves of car-body free-form surface, and new control points require to be added onto the surface through surface refinement in many cases for modeling the required LFL. When refining the Bezier surface through order-elevation or NURBS surface via knot-insertion, new control points must be added in full rows or columns due to the rigid tensor-product scheme of Bezier surface and NURBS surface, and many of these newly added points are useless for the LFL modelling.

Classical deformation methods for free-form surface can be utilized to facilitate the LFL modelling in car-body styling design in two ways: geometry-based or mechanics-dependant. In geometric deformation methods, surface smoothness is formulated as useful geometry criteria in [28] to determine the shape deformation of surface by solving a constrained variational optimization problem. In [5], a set of geometry constraint points are defined over surface to control the deformation editing. Each geometry constraint point has a desired displacement as well as an influence region determined by B-spline basis function. Among mechanical deformation approaches, Lagrangian mechanics is incorporated with NURBS in [27] to produce a so-called D-NURBS surface, which can be deformed by applying virtual forces and shape constraints. In [22], a mechanical model based on Force Density Method [16] is introduced to drive the deformation of B-spline surface, by imposing virtual forces onto a bar network which is coupled with the control polygon of freeform surface.

After completing the car-body styling design through LFL modeling, finished CAD model needs to be imported into CAE application for mechanical analysis, so as to check the feasibility of product design in engineering. However, CAD and CAE have the issue of data incompatibility thanks to their different model descriptions, and one CAD model always requires to be converted into another CAE-suitable model before applying engineering analysis. Such a CAD-to-CAE conversion process is normally cumbersome and time-consuming, which severely affects the smooth integration between styling design and mechanical analysis in automotive design. Fortunately, a new development in computational mechanics offered a powerful technology called the isogeometric analysis (IGA) [12], which has the capability of seamlessly integrating CAD and CAE models with a unified mathematical framework. In CAE field, IGA technology has been extensively used to handle many complex engineering analysis problems directly based on CAD models, such as the shell analysis [4][15], structural vibration [7], fluid mechanics and electromagnetics [8], composite structure [9], aerodynamics [10], etc.

T-splines [26] is an advanced geometry description in CAD field and is good at defining complex freeform surfaces with compact control points. In comparison with other popular CAD geometries like Bezier surface, B-spline surface and NURBS surface, T-splines has a less rigid surface structure by allowing the addition of T-junctions through flexible local refinements. Unidirectional T-splines (UT-splines) is a subset of T-splines that has either vertical T-junctions or horizontal T-junctions. It is due to such a one-directional surface structure that makes UT-splines have the unique advantage in some aspects of surface modeling, especially in surface skinning. Aided by UT-splines, the approximate skinning method [29], local skinning method [19], improved local skinning method with shape preservation [21], and the skinning method guided by curves [11] have been developed in recent years to improve the popular surface skinning algorithm in CAD field, which is extensively utilized in shipbuilding, automotive and aviation industries. Except for surface skinning, UT-splines also has the advantage in computer aided styling design of automotive vehicle, since its one-directional structure is very helpful to the LFL modeling of car-body freeform surface along isocurves, as seen in Figure 1.

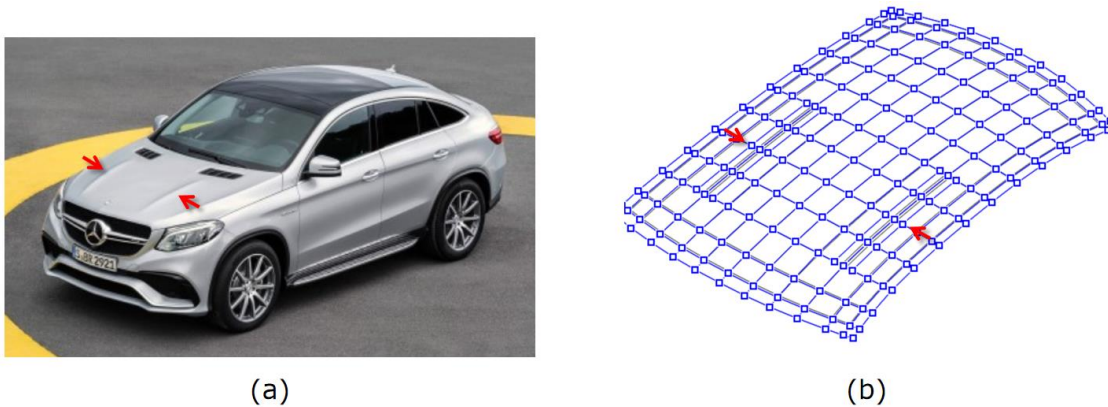


**Figure 1:** The similarity between car-body surface (courtesy of Mercedes Benz) with LFLs (a) and UT-splines structure (b).

In this paper, we introduce a new LFL modeling approach for car-body freeform surface on the basis of UT-splines and IGA. This approach employs UT-splines to achieve the efficient creation of LFL through local refinements first. Then, thin-shell theory is incorporated into UT-splines by means of IGA, producing an UT-splines+ in which CAD and CAE models fuse together. With UT-splines+, LFL can be further flexibly modified by using virtual forces from CAE model through mechanical editing. Moreover, UT-splines+ offers more capabilities to LFL modeling on car-body surface, by enabling the styling design and mechanical analysis to be done simultaneously.

This paper is organized as follows and we restrict our discussion on the case of bicubic T-splines and UT-splines. First, we describe the UT-splines and T-splines in Section 2. In Section 3, we investigate the inherent analysis-suitability of UT-splines. Section 4 details the construction of UT-splines+ and how the mechanical property of UT-splines+ facilitates the surface modelling and engineering analysis. In Section 5, a specific case study on car bonnet design is offered to demonstrate the effectiveness of our proposed approach. Finally, Section 6 concludes the paper.

In particular, NURBS surface, UT-splines and UT-splines+ will be distinguished from each other in this paper by having the black, green and red control points, respectively.

## 2 T-SPLINES AND UT-SPLINES

T-splines is an advanced mathematical description to define freeform surface in CAD field. Different from the popular tensor-product scheme of NURBS surface, T-splines adopts the formulation of point-based splines [26] and is defined over a two-dimensional T-mesh that allows for flexible T-junctions. By means of a straightforward ray-tossing method [26], each B-spline function  $B_i$  of T-splines deduces its local knot vector of  $(s_{i_0}, s_{i_1}, s_{i_2}, s_{i_3}, s_{i_4}) / (t_{i_0}, t_{i_1}, t_{i_2}, t_{i_3}, t_{i_4})$  from T-mesh topology. Figure 2(a) shows a common T-mesh structure with 12 T-junctions from  $T_1$  to  $T_{12}$ , and the B-spline function  $B_6$  anchored at  $T_6$  is locally defined over a knot vector of  $(s_{60}, s_{61}, s_{62}, s_{63}, s_{64}) / (t_{60}, t_{61}, t_{62}, t_{63}, t_{64})$ . After all the B-spline functions determine their local knot vectors from T-mesh and a group of control points  $P_i$  are given to form a control polygon, T-splines can be mathematically defined through Equation (2.1).

$$P(s, t) = \sum_{i=0}^n P_i \times B_i(s, t) \tag{2.1}$$

Based on the types of T-junctions in T-splines, we can divide T-splines into the common T-splines and UT-splines, as seen in Figure 3. Common T-splines is defined upon a T-mesh having both vertical and horizontal T-junctions, such as the one in Figure 2(a). Yet, UT-splines is defined over a T-mesh that merely permits one type of T-junction, either vertical or horizontal ones. Figure 2(b) shows a T-mesh for UT-splines that only has horizontal T-junctions. The B-spline function  $B_4$  at  $T_4$  deduces its local knot vector of  $(s_{40}, s_{41}, s_{42}, s_{43}, s_{44}) / (t_{40}, t_{41}, t_{42}, t_{43}, t_{44})$  through ray-tossing method. In contrast with common T-splines, UT-splines has some advantages in surface construction and isogeometric analysis.

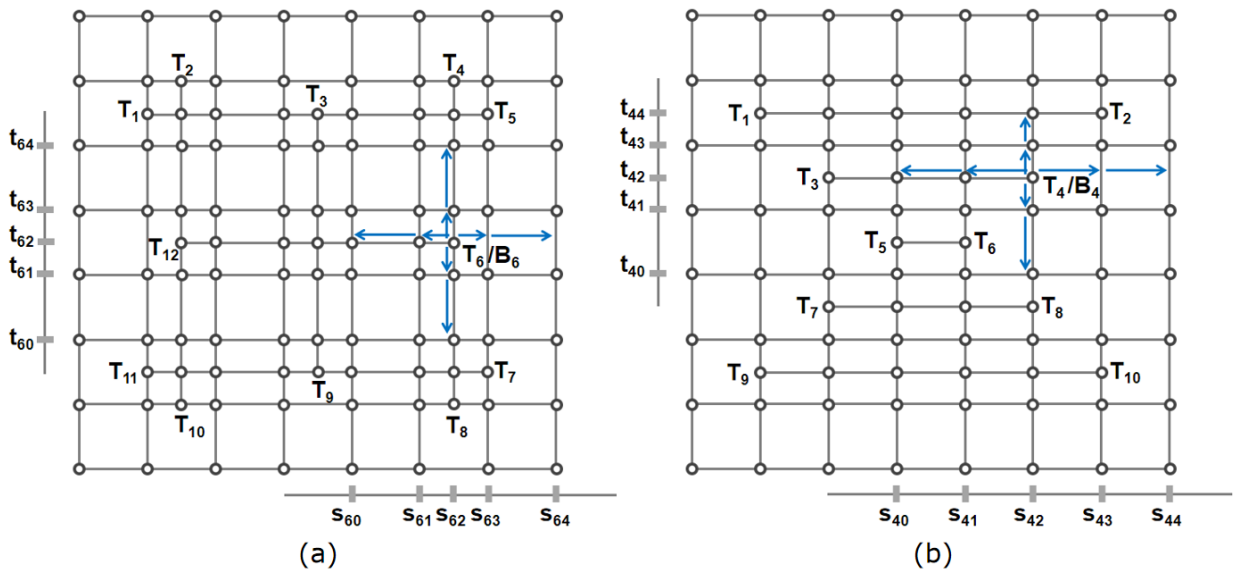


**Figure 2:** T-meshes for common T-splines (a) and UT-splines (b), respectively.

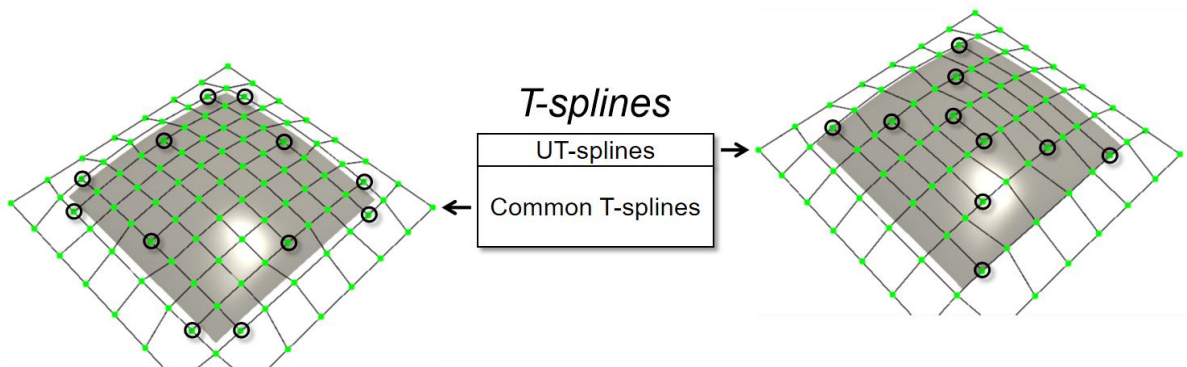


**Figure 3:** The classification of T-splines and black circles indicate T-junctions.

First, UT-splines are much easier to construct than common T-splines. The basic refining algorithm of T-splines was introduced in [26], and then a more flexible refining algorithm was proposed in [25] soon after. To get the target T-mesh shown in Figure 4(a) for one UT-splines, new junctions can be freely added onto an initial uniform mesh by repeatedly applying local refining algorithm, without caring about specific refining strategy. However, if we want to obtain the T-mesh seen in Figure 4(b) for one common T-splines, we not only need to carefully select proper refining strategy during local refinements, but also have to add many other wanted junctions onto T-mesh as seen in Figure 4(c), which involves an intricate refining process.

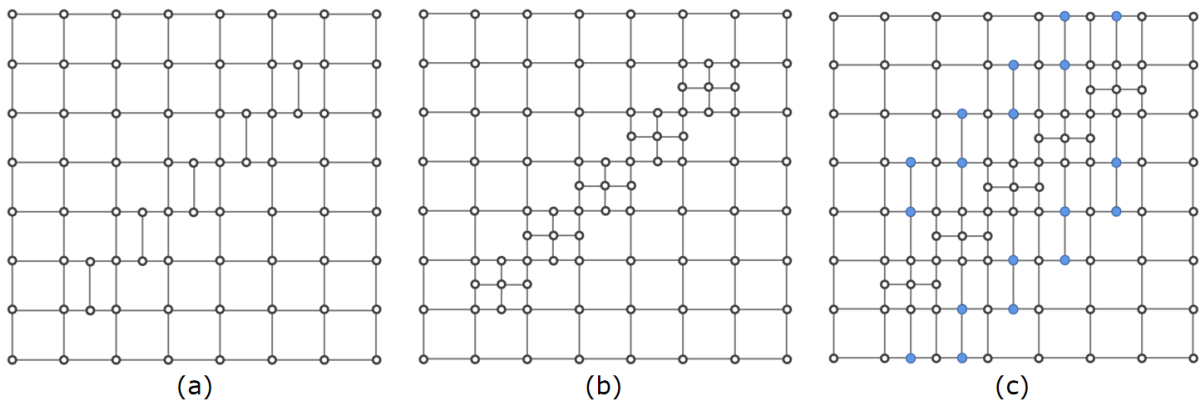


**Figure 4:** The comparison of construction difficulty between UT-splines and T-splines: (a) Target T-mesh for UT-splines, (b) Target T-mesh for common T-splines, (c) Resulting T-mesh with 18 redundant junctions in blue.

Except for the easiness in construction, UT-splines also has the advantage in IGA over common T-splines for its inherent analysis-suitability, which will be investigated in next section.

### 3 ANALYSIS-SUITABILITY OF UT-SPLINES

Because not all the T-spline surfaces are guaranteed to be linearly independent [6], T-spline surfaces need to be checked for the analysis-suitability before being used in IGA applications. Computing the nullity of T-splines-to-NURBS transformation matrix is a reliable way to determine the linear independent property of T-splines [17]. Yet, the whole computation process is cumbersome, since many local refinements need to be applied. A simple topology condition for T-mesh was also proposed in [17] and can be applied to intuitively visualize the linear independence of T-splines. Here, we adopt this topology-based approach to verify the inherent analysis-suitability of UT-splines.

Over T-mesh, T-extension can be defined for each T-junction by extending two edges forward and one edge back from that T-junction. For example, there are six vertical and six horizontal T-extensions on the T-mesh in Figure 5(a), where each T-extension has two yellow edges forward and one purple edge back. If no horizontal T-extension intersects the vertical T-extension over one T-mesh, the linear independence property can be guaranteed for T-splines. Because UT-splines has either vertical or horizontal T-junctions, T-extensions over its T-mesh are parallel or overlapped all the time and never intersect, like the one in Figure 5(b). Therefore, UT-splines is always linearly independent to be suitable for IGA.

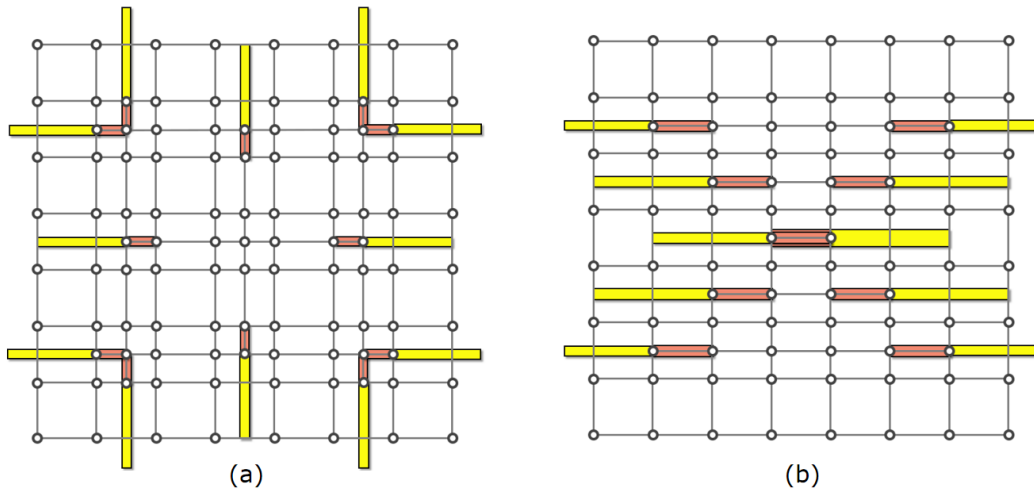


**Figure 5:** The distribution of T-extensions on the T-meshes of common T-splines (a) and UT-splines (b).

By contrast, common T-splines requires to carefully select proper refining strategy during local refinements to ensure the analysis-suitability, such as the analysis-suitable refining algorithms proposed in [18] and [24].

#### 4 UT-SPLINES+ WITH MECHANICAL PROPERTY

Thin-walled structures are extensively used in automotive industry, thanks to their impressive performance in car-body lightweight design. In computational mechanics, mechanical analysis of thin-walled structure has been one of the most important issues and is commonly realized in CAE field based on the classical Kirchhoff-Love shell theory. In recent years, isogeometric shell analysis through CAD geometry has been developed to improve existing thin-shell analysis methods, and can be more efficiently done with better solutions [4][15] than those traditional methods relied on finite element mesh model. It is because that the necessary continuities between shell elements can be more easily ensured in IGA than FEA. Moreover, CAD geometry can be exactly reused in IGA for mechanical analysis, instead of being converted to another inaccurate polygon mesh for analysis.

Here, we apply isogeometric Kirchhoff-Love shell analysis method [15] to convert UT-splines into another UT-splines+ that has additional mechanical property. The details relating to specific computer implementation can be found in [20]. After the conversion, surface geometry of UT-splines+ is still described by Equation (2.1) and the displacement field for mechanical analysis on UT-splines+ is defined through Equation (4.1), in which  $X_i$  represents the displacement value occurring at the control point  $P_i$  after external force is applied.

$$D(s,t) = \sum_{i=0}^n X_i \times B_i(s,t) \quad (4.1)$$

From Equation (2.1) and Equation (4.1), a same set of B-spline functions  $B_i(s,t)$  are used to define both the surface equation  $P(s,t)$  in CAD and the displacement field  $D(s,t)$  in CAE, unifying the design and analysis models with a same mathematical description. Figure 6 shows the

conversion process from one purely geometric UT-splines to another UT-splines+ having mechanical property.

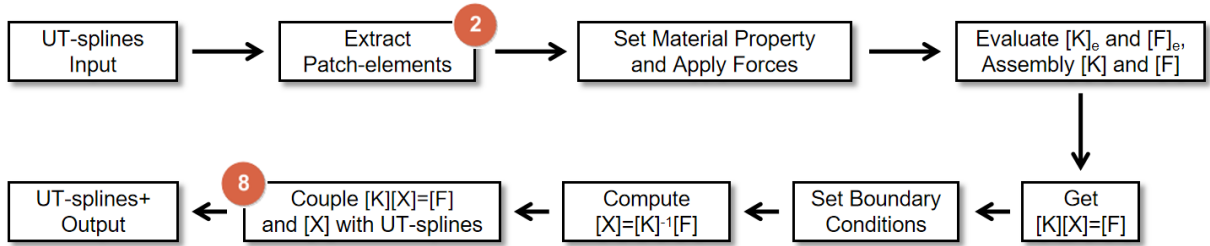


**Figure 6:** The conversion from UT-splines to UT-splines+ with the aid of IGA.

From Figure 6, we can see that UT-splines+ has an additional analysis model compared to the initial UT-splines. This analysis model is built entirely based on the patch-elements of UT-splines itself in Step 2, instead of being established over the mesh-elements that result from the costly mesh generation of UT-splines. In Step 8, we link the global stiffness matrix equation  $[K][X]=[F]$  with UT-splines and assign each displacement value  $X_i$  in  $[X]$  which is computed from this matrix equation to corresponding control point  $P_i$ , producing the UT-splines+ that will make following surface modeling and engineering analysis easier.

For example, we set the material property along with the boundary condition, and apply the forces over the UT-splines+ in Figure 7(b) that is converted from an initial UT-splines in Figure 7(a), obtaining the computed displacement value  $X_i$  in  $[X]$  at each control point  $P_i$ . Then, we can opt to achieve the flexible mechanical deformation design of UT-splines+ through  $[X]$  by simply updating each  $P_i$  with its assigned displacement value  $X_i$ , resulting in an intuitive mechanical editing effect in CAD caused by virtual forces in Figure 7(c). Or, we can also choose to realize the direct mechanical analysis in CAE without applying mesh generation over UT-splines+ at this time, by carrying out the post-processing of  $[X]$  to generate the Von-Mises stress result shown in Figure 7(d). Therefore, UT-splines+ with mechanical property will have more capabilities than UT-splines in both CAD and CAE applications.

## 5 CASE STUDY

In this section, we will demonstrate the effectiveness of our new LFL modeling approach aided by UT-splines and IGA, based upon a specific modeling example of car bonnet in automotive design.

First, we exactly convert bonnet surface from the popular NURBS surface in Figure 8(a) to a special class of T-splines without T-junctions in Figure 8(b), by redefining B-spline functions of NURBS surface over a uniform T-mesh through ray-tossing method. Although the converted T-splines has the same shape as initial NURBS surface, bonnet surface after the conversion possesses the flexible local refinability. Then we can refine the surface through local refinements as seen in Figure 8(c) to locally add 20 new control points along the isocurves, resulting in an UT-splines ready for subsequent LFL modeling. If we refine the bonnet surface in the form of NURBS surface along same isocurves, we have to add 96 control points onto surface in full columns in Figure 8(d) due to the rigid tensor-product structure of NURBS surface.

With UT-splines, we can achieve an efficient LFL modeling for bonnet surface by editing control points near isocurves, based on a compact UT-splines geometry rather than a cumbersome NURBS geometry. As seen in Figure 9(a), all the new points locally added onto UT-splines take part in modeling the LFLs to achieve the required aesthetically dynamic effect of bonnet surface. However,

as seen in Figure 9(b), most of new points that are added onto NURBS surface after refinements are useless for LFL modeling and they make the NURBS geometry complex and cumbersome. In addition, UT-splines are more suitable than common T-splines, which allows for T-junctions in both directions, for modeling these LFLs along isocurves over the bonnet surface with its simple one-directional surface structure.

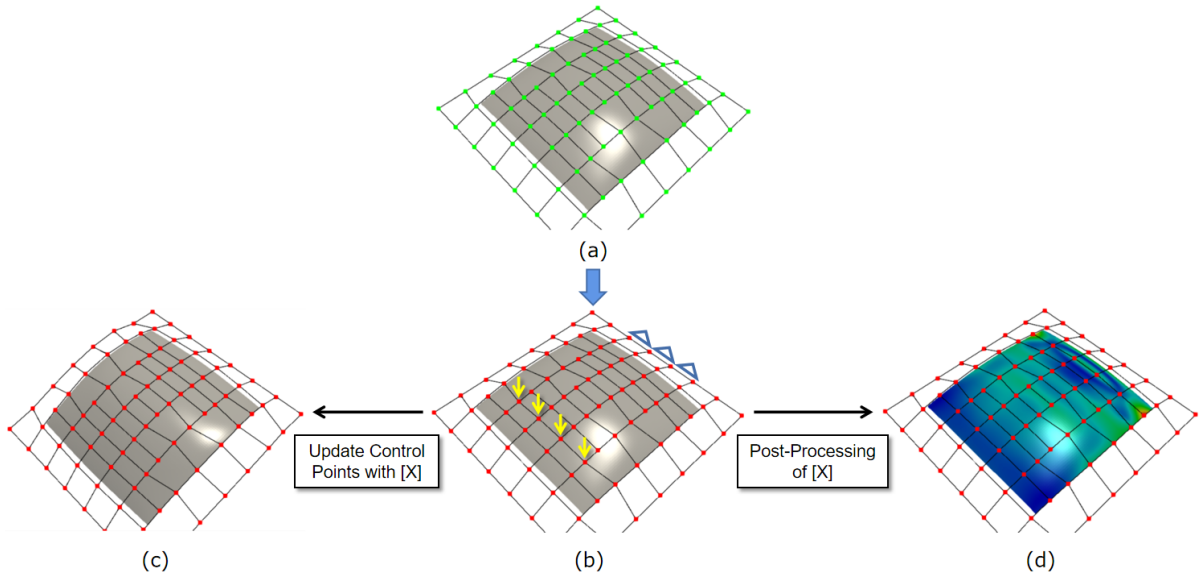


**Figure 7:** UT-splines+ for modeling and analysis: (a) Initial UT-splines, (b) Converted UT-splines+, (c) Mechanical deformation of UT-splines+, (d) Mechanical analysis of UT-splines+.

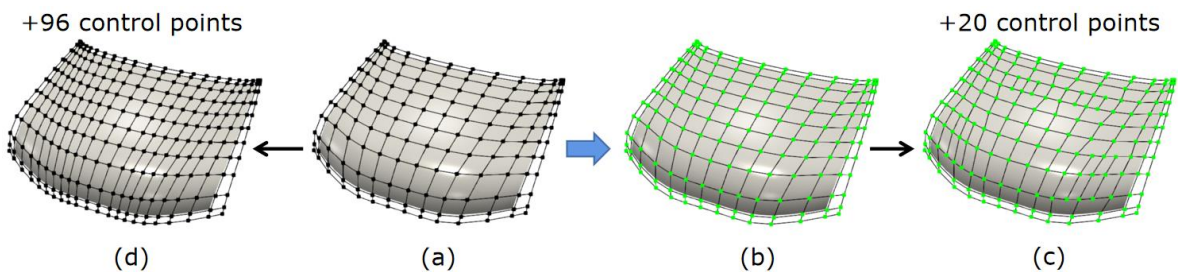


**Figure 8:** The conversion and refinement of bonnet surface : (a) NURBS surface, (b) Converted T-splines, (c) Resulting UT-splines from local refinements, (d) Fully refined NURBS surface.

Next, we convert the bonnet surface in purely geometric UT-splines in Figure 10(a) to another UT-splines+ having mechanical property in Figure 10(b), by applying isogeometric Kirchhoff-Love shell analysis as described in Section 4 to fuse the design model and analysis model seamlessly within UT-splines+. In this way, we can utilize the embedded analysis model to facilitate subsequent surface modeling as well as engineering analysis over bonnet surface.

In Figure 11(a), we keep four boundaries fixed and set the material property for UT-splines+, so that we can flexibly modify the LFLs through intuitive mechanical editing. As seen in Figure 11(b), we apply pulling forces at two control points located in the centers of lower LFLs, and control points over the front end of bonnet surface are driven by the thin-shell analysis model in UT-splines+ to move naturally in coordination, quickly obtaining a new styling design for bonnet.



In Figure 11(c), we continue to apply pushing forces at four control points that locate in the middle of two upper LFLs, and neighbouring control points automatically move in groups also according to the underlying analysis model of UT-splines+, producing a final bonnet surface that is more attractive than the initial one in Figure 11(a).

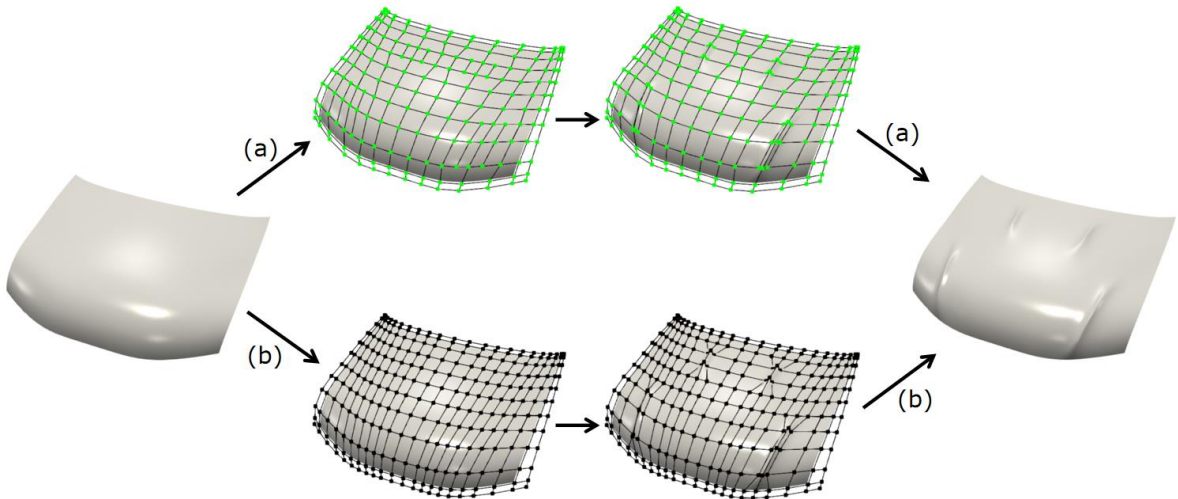


**Figure 9:** LFL modeling on bonnet surface : (a) Modeling procedure based upon the UT-splines with compact control points, (b) Modeling procedure based on the refined NURBS surface that has many redundant control points.

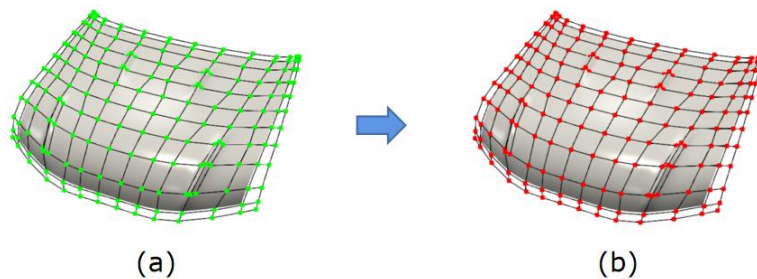


**Figure 10:** The conversion of bonnet surface from the UT-splines (a) with only geometry information to the UT-splines+ (b) having additional mechanical property.

If we choose geometric editing to modify these existing LFLs, it is not easy to achieve the same design effect as in the case of applying mechanical editing. For example, in Figure 12(b), we move the same two control points upwards as in Figure 11(b) through geometric editing, LFLs can be only altered to become sharper and lose some sense of beauty. In Figure 12(c), we move those identical four control points downwards in a same way as in Figure 11(c) via geometric editing, the altered LFLs result in a poor design effect with no sharpness. Even if we can finally realize a LFL modeling result similar to Figure 11(c) using geometric editing, the entire modeling process will be laborious and time-consuming, because we need to manually adjust many control points in a very careful way. Hence, mechanical editing offered by UT-splines+ makes it more flexible to build the required LFL over bonnet surface than geometric editing.

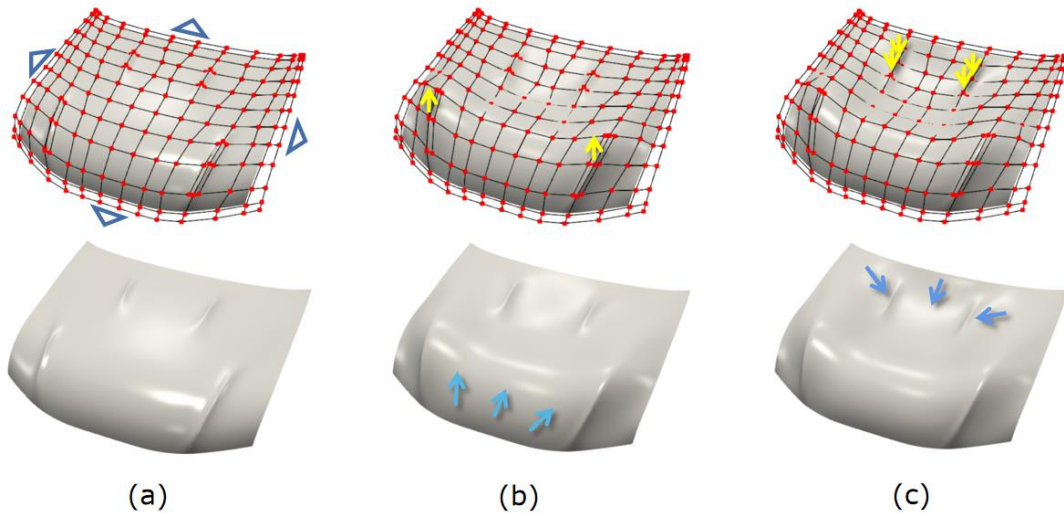


**Figure 11:** Flexible mechanical editing of bonnet surface through mechanical deformation: (a) Surface to be edited, (b) First mechanical alteration, (c) Second mechanical alteration.

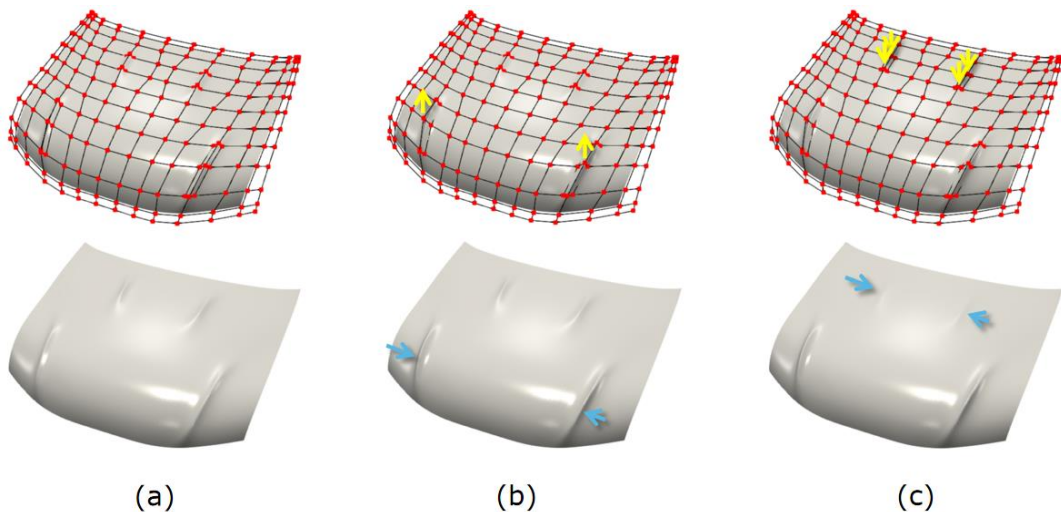


**Figure 12:** Inflexible geometric editing of bonnet surface via geometric manipulation : (a) Surface to be edited, (b) First geometric modification, (c) Second geometric modification.

In addition, we can enable the LFL modeling in styling design and the mechanical analysis in engineering to be performed simultaneously also based on UT-splines+, whose analysis and design models have been seamlessly merged together. As seen in Figure 13(a), bonnet surface needs to be altered twice during styling design reviews to meet constantly changing design requirements. In Figure 13(b), UT-splines1+ is the initial design, and UT-splines2+ is produced from UT-splines1+ by adding four LFLs via geometric editing, and UT-splines3+ is obtained from UT-splines2+ by modifying these LFLs with virtual forces through mechanical editing. UT-splines1+ to UT-splines3+ represent three different design styles for bonnet surface.

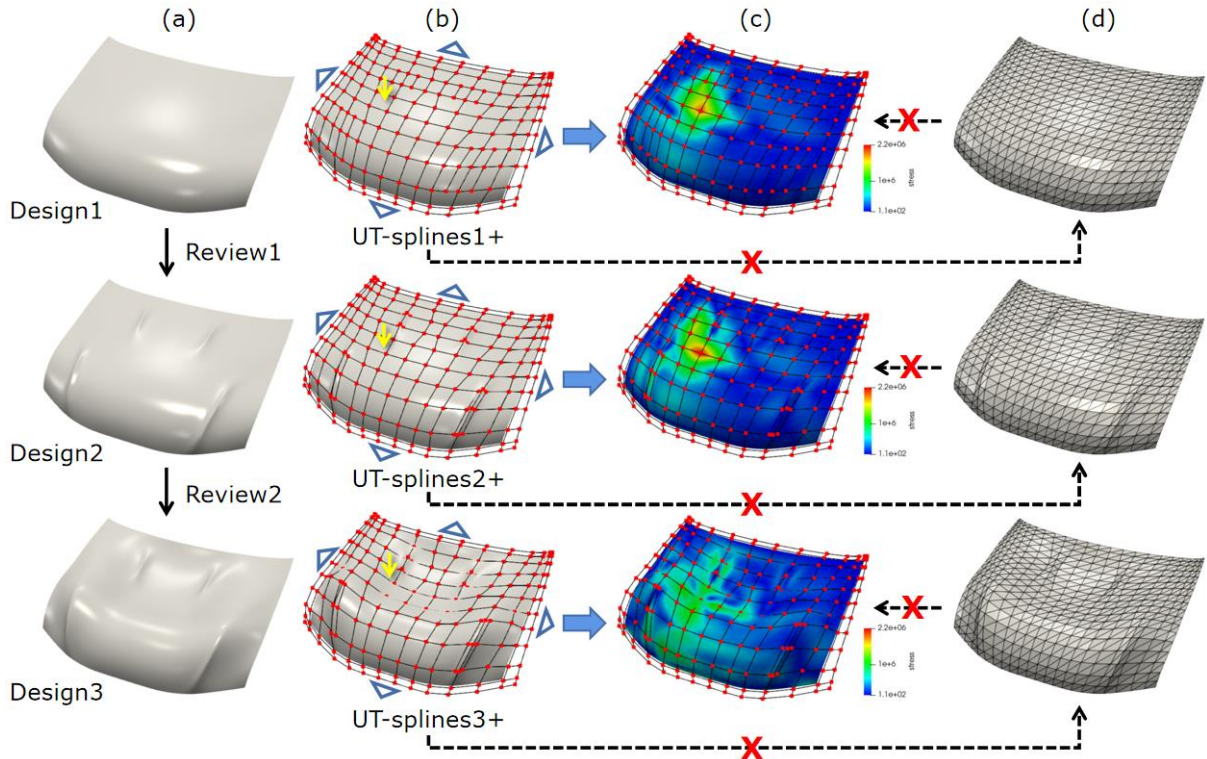


**Figure 13:** The comparison of CAD-to-IGA workflow and CAD-to-FEA workflow in design reviews : (a) Designs for bonnet surface, (b) UT-splines+ for different designs, (c) Different mechanical analysis results, (d) Corresponding finite element models after meshing.

To check the engineering feasibility of these bonnet designs, we set identical boundary condition and material property on those UT-splines+ in Figure 13(b), and then conduct a simple impact simulation analysis caused by a falling object to verify the stiffness performance of car bonnet. Because thin-shell mechanical property based on Kirchhoff-Love theory has been blended into UT-splines+ through IGA, we can thus quickly obtain the analysis results in Figure 13(c) directly on CAD geometry, after modifying the shape of UT-splines+ to get a new style design each time. We do not need to convert UT-splines+ into complicated finite element analysis (FEA) models shown in Figure 13(d) before applying mechanical analysis to bonnet surface in CAE.

Therefore, UT-splines+ can ensure a simultaneous mechanical analysis while modeling the LFLs on bonnet surface through such a new CAD-to-IGA workflow, offering a more practical tool for designers to use in automotive styling design than the traditional designing tool based on tedious and time-consuming CAD-to-FEA workflow.

## 6 CONCLUSION

This paper introduces a new approach for modeling the LFL on car-body surface in automotive styling design, with the help of UT-splines and IGA. First, UT-splines with a simple one-directional surface structure is applied to achieve the efficient LFL modeling by means of local refinements along isocurves. Kirchhoff-Love shell theory is then incorporated into UT-splines via IGA to generate a UT-splines+ that has a seamlessly merged design-analysis model. On the basis of UT-splines+, LFL can be more flexibly modeled over car-body surface by using virtual forces through mechanical editing. Additionally, LFL modeling in CAD also becomes more practical in engineering

by coupling mechanical analysis and styling design through the new CAD-to-IGA workflow offered by UT-splines+. A bonnet design case is given in the end to demonstrate the effectiveness of our proposed new LFL modeling approach for automotive designers.

In this paper, all the design examples about car bonnet are realized based on our in-house codes that are built from scratch with OpenGL and Paraview. Next, we will study how to implement UT-splines and UT-splines+ within one commercial CAD system like the RhinoCAD [23], so as to develop a more useful LFL modeling tool for automotive designers in practical applications.

Xiang Xue, <https://orcid.org/0000-0001-6125-3122>

## REFERENCES

- [1] Alias Auto, <https://www.autodesk.com/products/alias-products/features>, Autodesk.
- [2] Aoyama, H.; Miyauchi, S.; and Sakai, Y.: Construction of basic shape with character lines for car body design by image language (Kansei Language), Futureground - DRS International Conference 2004, 17-21 November, Melbourne, Australia.  
<https://dl.designresearchsociety.org/drs-conference-papers/drs2004/researchpapers/70>
- [3] Bazilevs, Y.; Calo, V.M.; Cottrell, J.A.; Evans, J.A.; Hughes, T.J.R.; Lipton, S., Scott, M.A.; Sederberg, T.W.: Isogeometric analysis using T-splines, *Computer Methods in Applied Mechanics and Engineering*, 199(5-8), 2010, 229-263.  
<https://doi.org/10.1016/j.cma.2009.02.036>.
- [4] Benson, D.J.; Bazilevs, Y.; Hsu, M.C.; Hughes, T.J.R.: Isogeometric shell analysis: The Reissner-Mindlin shell, *Computer Methods in Applied Mechanics and Engineering*, 199(5-8), 2010, 276-289. <https://doi.org/10.1016/j.cma.2009.05.011>.
- [5] Borrel P.; Rappoport A.: Simple constrained deformations for geometric modeling and interactive design, *ACM Transactions on Graphics (TOG)*, 13(2), 1994, 137-155.  
<https://doi.org/10.1145/176579.176581>
- [6] Buffa, A.; Cho, D.; Sangalli, G.: Linear independence of the T-spline blending functions associated with some particular T-meshes, *Computer Methods in Applied Mechanics and Engineering*, 199(23-24), 2010, 1437-1445. <https://doi.org/10.1016/j.cma.2009.12.004>.
- [7] Cottrell, J.A.; Reali, A.; Bazilevs, Y.; Hughes, T.J.R.: Isogeometric analysis of structural vibrations, *Computer Methods in Applied Mechanics and Engineering*, 195(41-43), 2006, 5257-5296. <https://doi.org/10.1016/j.cma.2005.09.027>.
- [8] Garcia, D.; Pardo, D.; Calo, V. M.: Refined isogeometric analysis for fluid mechanics and electromagnetics, *Computer Methods in Applied Mechanics and Engineering*, 356, 2019, 598-628. <https://doi.org/10.1016/j.cma.2019.06.011>.
- [9] Hao, P.; Yang, H.; Wang, Y.T.; Liu, X.X.; Wang, B.; Li, G.: Efficient reliability-based design optimization of composite structures via isogeometric analysis, *Reliability Engineering & System Safety*, 209, 2021, 107465. <https://doi.org/10.1016/j.ress.2021.107465>.
- [10] Hsu, M.-C.; Akkerman, I.; Bazilevs, Y.: High-performance computing of wind turbine aerodynamics using isogeometric analysis, *Computers & Fluids*, 49(1), 2011, 93-100.  
<https://doi.org/10.1016/j.compfluid.2011.05.002>.
- [11] Hu, C.F.; Ai, J.M.; Lin, H.W.: Curve guided T-spline skinning for surface and solid generation, *Computers & Graphics*, 90, 2020, 84-94. <https://doi.org/10.1016/j.cag.2020.05.021>.
- [12] Hughes, T.J.R.; Cottrell, J.A.; Bazilevs, Y.: Isogeometric analysis: CAD, finite elements, NURBS, exact geometry and mesh refinement, *Computer Methods in Applied Mechanics and Engineering*, 194(39-41), 2005, 4135-4195. <https://doi.org/10.1016/j.cma.2004.10.008>.
- [13] ICEM Surf, <https://www.3ds.com/products-services/catia/products/icem-surf/>, Dassault Systèmes.
- [14] Katsoulis, T.; Wang, X.; Kaklis, P.D.: A T-splines-based parametric modeller for computer-aided ship design, *Ocean Engineering*, 191, 2019, 106433.  
<https://doi.org/10.1016/j.oceaneng.2019.106433>.

- [15] Kiendl, J.; Bletzinger, K.-U.; Linhard, J.; Wüchner, R.: Isogeometric shell analysis with Kirchhoff–Love elements, *Computer Methods in Applied Mechanics and Engineering*, 198(49–52), 2009, 3902–3914. <https://doi.org/10.1016/j.cma.2009.08.013>.
- [16] Léon J.C.; Trompette P.: A new approach towards free-form surfaces control, *Computer Aided Geometric Design*, 12(4), 1995, 395–416. [https://doi.org/10.1016/0167-8396\(94\)00022-K](https://doi.org/10.1016/0167-8396(94)00022-K)
- [17] Li, X.; Zheng, J.M.; Sederberg, T.W.; Hughes, T.J.R.; Scott, M.A.: On linear independence of T-spline blending functions, *Computer Aided Geometric Design*, 29(1), 2012, 63–76. <https://doi.org/10.1016/j.cagd.2011.08.005>.
- [18] Morgenstern, P.; Peterseim, D.: Analysis-suitable adaptive T-mesh refinement with linear complexity, *Computer Aided Geometric Design*, 34, 2015, 50–66. <https://doi.org/10.1016/j.cagd.2015.02.003>.
- [19] Nasri, A.; Sinno, K; Zheng, J.-M.: Local T-spline surface skinning, *The Visual Computer*, 28, 2012, 787–797. <https://doi.org/10.1007/s00371-012-0692-1>
- [20] Nguyen, V.P.; Anitescu, C.; Bordas, S.P.A.; Rabczuk, T.: Isogeometric analysis: An overview and computer implementation aspects, *Mathematics and Computers in Simulation*, 117, 2015, 89–116. <https://doi.org/10.1016/j.matcom.2015.05.008>.
- [21] Oh, M.-J.; Roh, M.-I.; Kim, T.-W.: Local T-spline surface skinning with shape preservation, *Computer-Aided Design*, 104, 2018, 15–26. <https://doi.org/10.1016/j.cad.2018.04.006>.
- [22] Pernot, J.P.; Guillet, S.; Leon, J.C.; Giannini, F.; Catalano, C.E.; Falcidieno, B.: A shape deformation tool to model character lines in the early design phases, *Proceedings SMI. Shape Modeling International 2002. IEEE*, 2002, 165–276. <https://doi.org/10.1109/SMI.2002.1003542>
- [23] Rhino, <https://www.rhino3d.com/>, Robert McNeel & Associates.
- [24] Scott, M.A.; Li, X.; Sederberg, T.W.; Hughes, T.J.R.: Local refinement of analysis-suitable T-splines, *Computer Methods in Applied Mechanics and Engineering*, 213–216, 2012, 206–222. <https://doi.org/10.1016/j.cma.2011.11.022>.
- [25] Sederberg, T.W.; Cardon, D.L.; Finnigan, G.T.; North, N.S.; Zheng, J.M.; Lyche, T.: T-spline simplification and local refinement, *ACM Transactions on Graphics*, 23(3), 2004, 276–283. <https://doi.org/10.1145/1015706.1015715>
- [26] Sederberg, T.W.; Zheng, J.M.; Bakenov, A.; Nasri A.: T-splines and T-NURCCs, *ACM SIGGRAPH 2003*, 2003, 477–484. <https://doi.org/10.1145/1201775.882295>
- [27] Terzopoulos D.; Qin H.: Dynamic NURBS with geometric constraints for interactive sculpting, *ACM Transactions on Graphics (TOG)*, 13(2), 1994, 103–136. <https://doi.org/10.1145/176579.176580>
- [28] Welch, W.; Witkin, A.: Variational surface modeling, *ACM SIGGRAPH computer graphics*, 26(2), 1992, 157–166. <https://doi.org/10.1145/142920.134033>
- [29] Yang, X.N.; Zhang, J.M.: Approximate T-spline surface skinning, *Computer-Aided Design*, 44(12), 2012, 1269–1276. <https://doi.org/10.1016/j.cad.2012.07.003>.